A Study on the Rational Positioning of O-cell Boxes in Three Test Piles considering the Geology of Ho Chi Minh City, Vietnam

Lan Vu Hoang Bach
Faculty of Civil Engineering, University of Architecture Ho Chi Minh City, 196 Pasteur Street, District 3, Ho Chi Minh City, Vietnam
lan.bachvuhoang@uah.edu.vn (corresponding author)

Received: 4 January 2025 | Revised: 8 February 2025 | Accepted: 21 February 2025

 DOI: https://doi.org/10.48084/etasr.10123

ABSTRACT

The O-cell pile test has more advantages than the traditional loading test because it does not require a cumbersome reaction frame, counterweight, or anchor piling. Therefore, the cost of pile testing is dramatically reduced compared to top-down tests. The most essential aspect of the single-level bidirectional cell test is precisely determining the location of an O-cell box. This paper addresses inaccuracies in placing O-cells in bidirectional loading test results on full-scale, large-dimension, high-capacity barrettes test piles from three different projects in Ho Chi Minh City, Vietnam. Detailed analysis shows that the pile toe response is very small, the movement of the upper piles is relatively minor, and the skin friction along the pile segments is not fully mobilized. Research results indicate that the O-cells must be moved up to better predict the ultimate soil pile resistance. Therefore, the condition for placing the O-cell box at the load-balance plane is only a necessary condition. For better placement of the O-cell, the settlement-balance plane may be additionally considered as a sufficient condition and will be researched in future work.

Keywords-Osterberg pile test; position of O-cell box; pile loading test; modified unified method

I. INTRODUCTION

The calculation of pile bearing capacity [1] includes two components, shaft friction and toe response. These components are calculated based on soil physio-mechanical or capacity properties. These properties are not precise due to the sampling and laboratory testing processes, as well as the non-homogeneous nature of the soil. Numerous other methods include the two components and pile settlement [2, 3] to determine pile bearing capacity, but in situ tests are still needed to verify the soil properties. In-situ methods of determining pile bearing capacity such as load-test, Osterberg cell (O-cell) test, and strain gauges [4], are usually utilized. The O-cell tests seem very effective because they can provide both shaft friction and toe response, and they are used in many cases [5]. The tests are very effective in verifying the said analytical calculation.

The O-cell load test is a bi-directional axis, compressive, static load test conducted on a pile to evaluate the soil pile resistance and pile capacity. Osterberg developed this technique in 1987 [6], and founded the company Loadtest in 1991. Since then, more than 3,000 O-cell tests have been conducted worldwide. Authors in [7, 8] describe some of the many technical and economic advantages of the O-cell test, such as the fact that the O-cell test uniquely separates side shear from end bearing and the possible loading far exceeding top-down tests. A properly designed test that includes appropriate instrumentation should fully mobilize both the end bearing and the side resistance, as well as define the depth profile of side shear resistance. According to [9, 10], analysis of the test result provides an equivalent top-load curve for design based on the measured response of the separate components of capacity. The O-cell test can be a useful tool in the optimization of deep foundation design, which can result in significant economic savings compared to traditional loading tests.

The O-cell applies equal forces in opposite directions, including upward force to mobilize the skin friction of the pile above the cell and downward force to mobilize the end-bearing of the pile toe and the skin friction below the O-cell. Therefore, the pile-bearing capacity, determined from the test results, equals at least to the double of the load applied by the O-cell. When the location of the O-cell is not appropriate, the ultimate capacity of the pile section over the O-cell and the pile section under the O-cell are different because the unit shaft or unit base resistance is not fully mobilized. Therefore, the pile-bearing capacity obtained from this test is usually lower than the actual pile resistance. To optimize the test results, the O-cell should be positioned at a level where the shaft capacity of the upper section is approximately equal to both the end bearing and the shaft capacity of the lower section, e.g., at the load balance plane [11]. However, in practice, the balance of the bearing capacity of the upper and

lower sections of the pile cannot be reached. Some authors [2-4] propose simulating simultaneously the load-bearing and settlement behavior of piles with the neutral plane. This implies that the O-cell box needs to be positioned on this plane to achieve the most accurate load piles' bearing capacity.

This paper illustrates the process of analyzing the instrumented barrette piles and evaluates the location of the O-cell box placed in these piles under construction. It presents the test pile results, strain gauge evaluation, shaft resistance distribution, and correlation derived from the test results concerning the location of the O-cell box.

II. MATERIALS AND TEST PROGRAM

A. Test Piles Details and Soil Condition

1) Test Piles Details

Static load tests using single-level bidirectional cells were carried out for three barrette piles named TP1, TP2, and TP3, which were used for the deep foundations of the following projects: the Office Building Lim III, the Golden River Bason, and the Landmark 81 Tower, respectively. Figure 1 shows the locations of these buildings in Ho Chi Minh City, Vietnam.

Fig. 1. Locations of the three test piles in Ho Chi Minh City.

Table I shows the characteristics of the instrument piles. Bachy Soletanche Vietnam constructed the three barrettes and Fugro Singapore supervised the construction process.

TABLE I. DETAIL OF INSTRUMENTED TEST PILES

Item	TP1	TP2	TP3
Project	Lim III	Golden River Bason	Landmark 81
Length (m)	63	69	85
Cross-section area (mm)	2800×800	2800×800	2800×1000
Rebar number and size	54Φ32	44Φ32	38Φ32
Steel reinforcement ratio (%)	1.94	1.58	1.09
Concrete grade	B40	B40	B35
28-day concrete strength (MPa)	58	56.9	50.7
Length (m) above the cell	47	58	61.8
Length (m) below the cell	16	11	23.2
Buoyant weight above the cell (kN)	1500	1900	2400

All barrette test piles were constructed with rope grab excavation techniques with polymer slurry. The three test piles, i.e. TP1, TP2, and TP3, were drilled completely on October 27, 2017, February 5, 2016, and April 21, 2015, respectively. Each pile was instrumented with pairs of vibrating wire strain gauges at three or four levels below and five or six levels above the cell, as indicated in Figure 2.

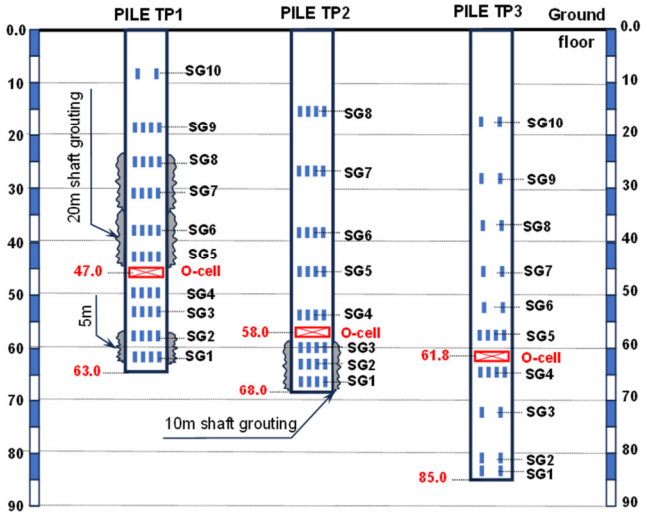

Fig. 2. Schematics of the O-cell test piles.

2) Site Sub-Surface Condition

The soil profile at the Lim III building (TP1) consisted of soft to medium-stiff sand, lean clay to about 9 m depth, loose to dense fine to medium sand extended to 37.2 m depth, followed by a 12.2 m thick layer of very stiff to hard fat clay and sandy lean clay. Hereunder, the soil profile consisted of fine to medium sand, dense to very dense to 77.8 m depth, underlain by hard fat clay, and sandy lean clay to 80 m depth (the end of the investigated borehole).

The site of the Vinhomes Bason project (TP2) consisted of filled sand to about 6.1 m deep, compacted loose sand up to 15 m depth, followed by a medium-density sand layer to 35.2 m depth, followed by very stiff to hard clay to about 63.2 m depth, and underlain by dense to very dense sand to at least 70 m depth.

The Saigon River (Figure 1) meandered and established the upper soil layer of the Landmark Tower (TP3). The subsurface stratigraphy at the general locations of the test barrettes is reported to consist primarily of organic silty clay to a depth of 28.7 m. Below the strata, sandy clay and dense to very dense sand was encountered to at least 90 m depth. Table II shows more details about the site sub-surface condition of three test piles.

B. Test Program

O-cell testing began by pressurizing the O-cell to break the task welds that hold it closed and to form the fracture plane in the concrete surrounding the base O-cell. Zero readings for all instruments were taken before the preliminary weld breaking.

According to [12-14], the O-cell tests of the three barrettes were conducted in 2 or 3 cycles, as follows:

- Pile TP1 was tested through two cycles, up to a maximum applied load of 38.78 MN in each direction, applied above and below the O-cell.
- Pile TP2 was also tested through two cycles, with the load reaching 17.1 MN and 32.02 MN, respectively.
- Pile TP3 was checked through three cycles. In cycle 1, the test pile was pressurized in four nominally equal increments, resulting in a maximum gross load of 18.1 MN in each direction applied above and below the O-cell. For cycles two and three, the O-cells were unloaded in six decrements and then reloaded with the same steps, reaching maximum loads of 33.9 MN and 41.9 MN, respectively.

TABLE II. SUB-SURFACE CONDITION DETAILS

TP1			TP2			TP3		
Zone	**Soil profile**	**SPT index**	**Zone**	**Soil profile**	**SPT index**	**Zone**	**Soil profile**	**SPT index**
Ground to SG10	Sandy Clay	11	Ground to SG8	Loose Sand	2	Ground to SG10	Organic Silty Clay	0
SG10 to SG9		11				SG10 to SG9		3
SG9 to SG8	Silty Sand	15	SG8 to SG7	Medium dense Sand	14	SG9 to SG8	Sandy Clay	21
SG8 to SG7		16				SG8 to SG7	Clayey Sand Dense, fine to medium Sand	29
SG7 to SG6		16	SG7 to SG6	Medium dense Sand	19	SG7 to SG6		29
SG6 to SG5		21	SG6 to SG5	Hard Clay	38	SG6 to SG5		30
SG5 to O-cell		29	SG5 to O-cell			SG5 to O-cell		36
O-cell to SG4	Sandy Clay	48	O-cell to SG4	Hard to very hard Clay	49	O-cell to SG4		37
SG4 to SG3		48	SG4 to SG3			SG4 to SG3	Dense, fine to medium Sand	55
SG3 to SG2	Silty Sand	43	SG3 to SG2	Dense Sand	64	SG3 to SG2		56
SG2 to pile base		45	SG2 to pile base			SG2 to pile base	Very Dense coarse Sand	83

III. TEST RESULTS

A. Load – Movement

The balance load is applied in the O-cell in two opposite directions, so it mobilizes pile resistance above and below the cell box. According to the theory, the cell does not impose an upward movement until its expansion force exceeds the buoyant weight of the pile above the cell (Table I). Figures 3 and 4 show the relationship between load and movement in the 2nd cycle of test piles TP1 and TP2, and TP3, respectively.

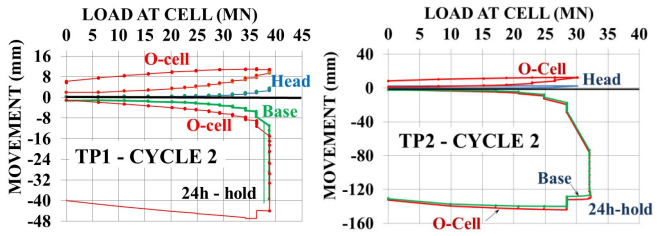

Fig. 3. Load – movement curves of TP1 and TP2 in Cycle 2.

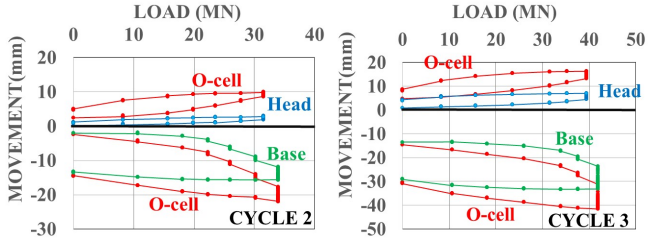

Fig. 4. Load – movement curves of TP3 in Cycle 2 and 3.

The test results show that the maximum movements of the three pile heads were 3.52 mm, 2.44 mm, and 7.03 mm, respectively. The upward movements of TP1 and TP2 are quite small, and smaller than those of the downward movements.

B. Load and Strain Measurements

Axial tangent stiffness (EA) is a vital parameter for converting the measured strain values to unit shaft resistance. For this case, we preferred to rely on the linear portions of load-strain relations and convert the measured strains using constant stiffness EA to determine the force by:

$$\sigma = Q/A = E\varepsilon \rightarrow Q = EA\varepsilon \quad (1)$$

where σ is the stress in the pile section, Q is the load in the pile section, A is the cross-section area of the pile, E is the Young modulus (elastic) of the pile material, and ε is the measured strain. Fellenius [15] proposes the tangent modulus method, which plots the graph of incremental strain versus the measured strain, as expressed in (2):

$$\Delta Q = EA \times \Delta\varepsilon \rightarrow EA = \Delta Q/\Delta\varepsilon \quad (2)$$

where $\Delta Q = Q_{i+1} - Q_i$ is the change of load from one load increment to the next and $\Delta\varepsilon = \varepsilon_{i+1} - \varepsilon_i$ is the change of strain from one load increment to the next.

The tangent modulus determined from the incremental stiffness procedure establishes the secant modulus relation that reduces with strain. Figure 5 describes the incremental stiffness plot for the gauge levels nearest the O-cell box for the second load cycle to TP1 and TP2. For these cases, we considered a constant stiffness (EA) of 72 GN and 70 GN for piles TP1 and TP2, respectively. Correlated to the nominal cross-sectional areas (2.24 m²), the values indicate that the E of the test barrettes is approximately 32 GPa and 31 GPa, respectively. The modulus of pile TP1 is larger than that of TP2, which may result in a different steel reinforcement ratios.

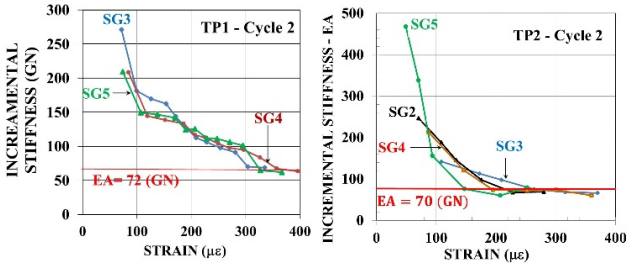

Fig. 5. Correlation of stiffness (EA) and strain of test piles TP1 and TP2.

Turning to the barrette test, the Fellenius method [15] was was applied TP3 to determine the pile stiffness EA value of 85 GN in cycle 3. For the nominal cross-sectional areas (2.8 m²), the values indicate that the *E* of this pile is approximately 31 GPa, which corresponds to the same value of TP2.

IV. RESULT ANALYSIS AND DISCUSSION

A. Analysis of the Test Data

1) Unit Shaft Resistance

The derived stiffness EA = 72 GN of pile TP1 was used to convert the averages of strain measured at each age level for each applied load (Q) in two-cycle loading tests by (1). The load distribution along the pile shaft is shown in Figure 6. The load distribution of the TP2 and TP3 also used the same sequence to determine the values at each strain gauge level. The load difference between the gauge levels is the shaft resistance between the pile and the soil. The value of the unit skin along the pile shaft can be determined with:

$$f_i = \frac{Q_i - Q_{i-1}}{uL_i} \quad (3)$$

where $Q_{i;}$ and Q_{i+1} represent the load at strain gage i and i+1, L_i is the length of the strain gauge i to the next, and u is the nominal pile perimeter.

The left and right diagrams of Figure 7 show the unit shaft resistance versus upward movement for some gage levels below and above the O-cell of the pile TP1. For test pile TP1, the skin unit below the cell level was fully mobilized at a movement of 8 mm to 10 mm and thereafter, shaft resistance became plastic. In contrast, the unit shaft friction of the pile segment (from SG6 to SG10) was relatively small and increased throughout the test. The movements of this pile portion conducted at these values are not likely sufficient to have fully mobilized the shaft resistance. The only pile portion between the O-cell and SG5 (located 3 m above the cell box) experienced upward movement greater than 10 mm, and the shaft resistance raised rapidly. Note that the pile segment from strain gage SG8 to the O-cell box used the shaft grouting technique to increase the skin resistance between the pile and the soil, but the result was unexpected.

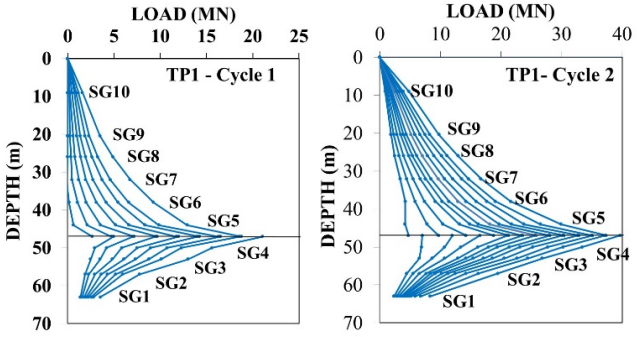

Fig. 6. Load distributions of TP1 in Cycles 1 and 2.

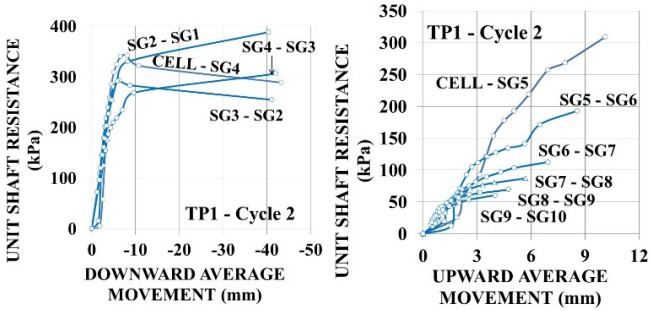

Fig. 7. Unit shaft resistance versus average movement of TP1.

Figures 8 and 9 describe the variation of unit friction based on data from the last loading cycle of test piles TP2 and TP3. Like the barrette test TP1, the skin unit of all pile segments below the O-cell reached the maximum value at downward movements of about 8 mm to 12 mm. After that, these values showed negligible change. The left graphs in Figure 8 show the maximum value of the unit skin of pile TP2, which ranges from 365 kPa to 340 kPa. Note that this pile segment used the shaft grouting technique to enhance the friction between the pile and the surrounding soils.

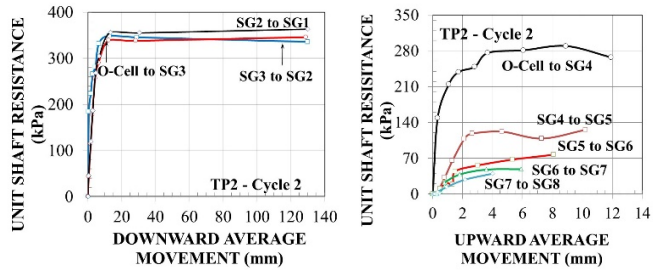

Fig. 8. Unit shaft resistance versus average movement of TP2.

Turning to the barrette TP3 (Figure 9), although the pile length is longer than that of TP2, the unit shaft resistance reached a peak of only 267 kPa. The corresponding values of almost all pile portions located at the upper cell level of TP2 and TP3 were quite small and raised throughout the experiment because the upward movements were rather minimal.

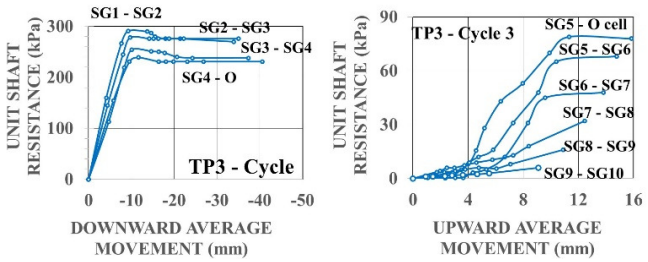

Fig. 9. Unit shaft resistance versus average movement of TP3.

2) Unit Base Resistance

The toe resistances of the test piles were not measured directly but were determined as the load at gage level SG1 (nearest the pile base) subtracted from the shaft resistance between gage levels SG1 and SG2. Thus, the unit base resistance of the three test piles was calculated with (4) and the results are shown in Table III.

$$q_b = \frac{Q_1 - (f_1 \times L_b)}{A_p} \quad (4)$$

where Q_1 is the load at strain gage 1 (SG1), f_1 is the unit skin friction of the pile segment from SG2 to SG1, L_b is the pile length from the SG1 to the toe, and A_p is the nominal pile area.

According to [1], the value of the unit base resistance in cohesionless soil can be predicted by using the SPT (Standard Penetration Testing) index based on Meyerhof's formula:

$$q_b = k_1 \times N_p \quad (5)$$

where q_b is the unit shaft and unit base resistance, k_1 is 120 for the bored pile, N_P is the average SPT index from 4D below the pile tip and 1D above the pile tip.

The unit base resistances of these test piles evaluated by strain gauge reports are smaller than those of theoretical values, which are predicted by (5). The results may be due to varying effects of the slurry filter cake around the pile tip or possibly varying pile cross-sections.

TABLE III. UNIT BASE RESISTANCE

Item	TP1	TP2	TP3
Unit base resistance determined by test data (kPa)	1060	3490	5940
The SPT index (N_p)	45	64	83
The value of unit base resistance evaluated by Meyerhof's formula (kPa)	5400	7680	9960

B. Discussion regarding the Position of the O-Cell Box

The unit shaft resistance of the three pile segments located above the O-cell of the test piles did not reach its ultimate value. Moreover, decreasing toe resistance made the capacity of the pile section located below the O-cell smaller than the corresponding value predicted by the theory. The results indicate that the location of the cell boxes needed to move upward to make more movement of the pile portion above the cell box and achieve balance between the capacity of the pile segments above and below the O-cell.

TABLE IV. THE NEW LOCATION OF CELL BOXES

Item	Unit	TP1	TP2	TP3
Ultimate shaft resistance	kN	42245	53958	91940
Base resistance determined by test data	kN	2345	7818	16632
Level of cell box (from the ground level)	m	- 43.1	- 48.6	- 57.1
Capacity of the pile segment above the cell box	kN	22295	30888	54286
Capacity of the pile segment below the cell box	kN	22295	30888	54286

The values of the base resistances were collected from the test results and the new location of the cell boxes was determined as shown in Table IV and Figure 10. The positions of the three O-cell boxes moved up by 3.9 m to 9.1 m, respectively, to balance the resistance of the upper and lower pile segments of each test barrette.

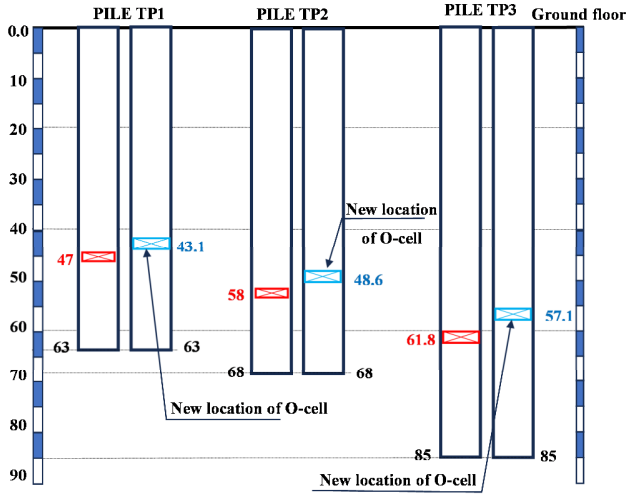

Fig. 10. Current and new location of the O-cell box of the three test piles.

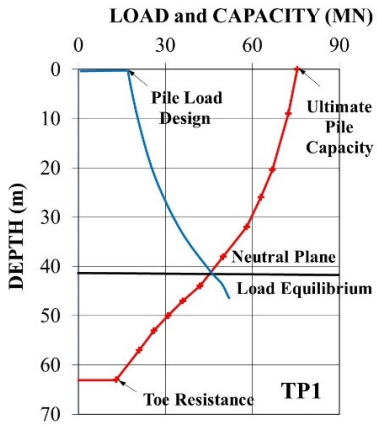

Fig. 11. Pile TP1 load and settlement compilation for the design.

Many researchers believe the O-cell box should be positioned at the load balance plane. Figure 11 shows the load balance plane that the design engineer likely assumed for the location of the O-cell box. It has shown that, with different

mobilizations of shaft and toe resistances, the location of the box should vary because the position of the plane is different.

Additionally, Figures 3 and 4 indicate that the movements of the pile head, pile base, and the overall movement of the O-cell boxes appear to coincide. Therefore, to position the box, the settlement balance plane may also need to be assessed and considered.

V. CONCLUSION

The curves of unit shaft resistance versus the upward movement of the three studied test piles showed that the shaft capacities of their upper pile segments were not fully mobilized because the movement between the surrounding soil and the upper pile segments was too small. Moreover, the unit base resistance of the three test piles determined by strain gauge data nearly equals 20% to 56% of the expected value. Depending on the impact of the drilling holes in the ground, the measured base capacity may be considerably reduced, therefore, the designers carefully consider determining the O-cell location to optimize bi-directional static load testing.

The O-cell boxes of the three barrettes constructed in Ho Chi Minh City were positioned on the load balance plane. However, this balance plane varies due to the applied test load and many other factors. Thus, the calculated bearing capacity is usually lower than its actual value. This study shows that placing the O-cell box at the load balance plane is challenging.

Future research should investigate the positioning of boxes not solely at the load-balance plane but also at the settlement-balance plane. Another avenue for exploration is the implementation of double cell box technology. These studies aim to achieve a more precise measurement of pile-bearing capacity via O-cell testing.

REFERENCES

[1] *TCVN 10304: 2014. Pipe Nail –Design Standards, Pile Foundation Design Standards*. TCVN, 2014.

[2] H. C. Van and T. A. Nguyen, "Numerical Simulation of Pile Design Method that Considers Negative Friction," *Civil Engineering and Architecture*, vol. 11, no. 5, pp. 2285–2292, Sep. 2023, https://doi.org/10.13189/cea.2023.110503.

[3] H. C. Van, "A Computer–Based Program for Pile Design with Consideration of Resistance Settlement, and Negative Friction Simultaneusly," *GEOMATE Journal*, vol. 26, no. 118, pp. 114–121, Jun. 2024.

[4] H. C. Van, "Pile Design using the Modified Unified Method combined with Monte Carlo Simulation," *Engineering, Technology & Applied Science Research*, vol. 14, no. 3, pp. 14275–14281, Jun. 2024, https://doi.org/10.48084/etasr.7247.

[5] J. Schmertmann, J. Hayes, T. Molnit, and L. Osterberg, "O-cell Testings Case Histories Demonstrate the Importance of Bored Pile (Drilled Shaft) Construction Technique," in *4th Conference of the International Conference on Case Histories in Geotechnical Engineering*, Mar. 1988, pp. 1–10.

[6] J. O. Osterberg, "The Osterberg load test method for bored and driven piles the first ten years," in *Seventh International Conference and Exhibition on Pilling and Deep Foundations*, Vienna, Austria, 1998.

[7] J. H. Schmertmann and J. A. Hayes, "The Osterberg cell and bored pile testing – A symbiosis," in *Third International Geotechnical Engineering Conference,* Cairo, Egypt, 1997.

[8] A. Ayithi, P. J. Bullock, H. S. Khoo, and G. V. Ramana, "Technical and Economic Benefits of O-cell load testing for deep Foundations in India," in *Indian Geotechnical Conference*, Roorkee, India, Dec. 2013, pp. 1–9.

[9] H.-J. Kim and J. L. C. Mission, "Improved Evaluation of Equivalent Top-Down Load-Displacement Curve from a Bottom-Up Pile Load Test," *Journal of Geotechnical and Geoenvironmental Engineering*, vol. 137, no. 6, pp. 568–578, Jun. 2011, https://doi.org/10.1061/(ASCE)GT.1943-5606.0000454.

[10] O. S. Kwon, Y. Choi, O. Kwon, and M. M. Kim, "Comparison of the Bidirectional Load Test with the Top-Down Load Test," *Transportation Research Record*, vol. 1936, no. 1, pp. 108–116, Jan. 2005, https://doi.org/10.1177/0361198105193600113.

[11] P. Dong, X. Wang, and H. Wang, "Study on the position of load box for pile foundation of Qilu Yellow River Approach Bridge," *IOP Conference Series: Earth and Environmental Science*, vol. 787, Jun. 2021, Art. no. 012120, https://doi.org/10.1088/1755-1315/787/1/012120.

[12] *Report on Barrette load testing Osterberg Method for Office Building LIM III*, Fugro Load Test Asia Pte. Ltd, Nov. 10, 2017.

[13] *Report on Barrette load testing Osterberg Method for Pile TN6 - Vincomes Bason*. Fugro Load Test Asia Pte. Ltd, 2016.

[14] *Report on Barrette load testing Osterberg Method for Landmark Tower*. Fugro Load Test Asia Pte. Ltd, 2015.

[15] B. H. Fellenius, *Basics of Foundation Design*, Electronic Edtition. Vero Beach, FL, USA: Pile Buck International, 2017.